Experimental Investigation of Charpy Impact Tests on Metallic SLM parts

E. Yasa, J. Deckers, J.-P. Kruth
Catholic University of Leuven, Belgium

M. Rombouts, J. Luyten
VITO NV, Mol, Belgium

ABSTRACT: Selective laser melting (SLM) is a layer-additive manufacturing technology making it possible to create fully functional parts directly from standard metal powders without using any intermediate binders or any additional post-processing steps. During the process, a laser source selectively scans a powder bed according to the CAD data of the part to be produced and powder particles are completely molten by a high intensity laser beam. SLM is capable of producing near full density metallic parts with an almost infinite geometric freedom. However, the mechanical properties obtained with SLM may differ from the ones of bulk material. In this study, Charpy impact tests are applied on the samples that were produced by SLM from different metallic powders; a titanium alloy Ti-6Al-4V, stainless steel 316L (X2CrNiMo18-14-3) and maraging steel 300 (X3CoMoTi18-9-5). The influence of building axis as well as of various heat treatments applied on the samples after SLM is investigated. The evolution of the microstructures of the sample parts is also studied.

1 INTRODUCTION

The of Selective Laser Melting (SLM) technology allows to obtain fully functional, three dimensional objects by selectively consolidating successive layers of powdered metal material on top of each other without using any intermediate binders or any additional post-processing steps [1]. Nowadays, Selective Laser Sintering/Melting technologies are widely used in various industries such as in medical, automotive and aerospace applications offering a range of advantages compared to conventional manufacturing techniques: shorter time to market, mass customization, geometrical freedom and ability to produce more functionality in the parts with unique design and intrinsic engineered features [1, 2].

During the SLM process, a powder layer is deposited onto a base plate attached to the building platform of the machine. The laser beam scans the powder bed according to the slice data of the CAD model, and the powder being fully molten forms the first layer on the base plate. Then, the building platform is lowered with an amount equal to the layer thickness and a fresh layer of powder is deposited on the already solidified layer. Successive scanning and lowering the building platform continues until the part is completely made. A typical SLM machine is shown schematically in Figure 1 with its main components.

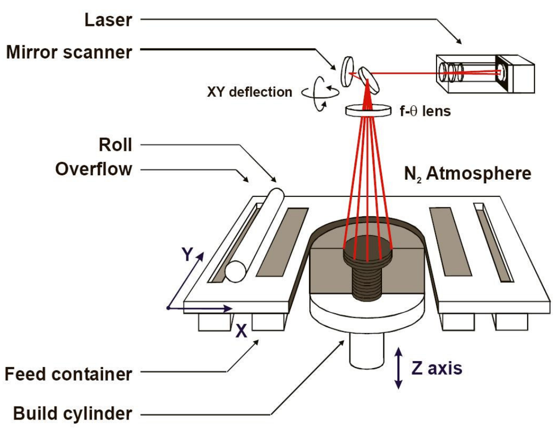

Figure 1: A typical SLM machine layout

The mechanical properties obtained with SLM might be different than the ones of bulk material produced by conventional techniques due to several reasons. Laser processing of materials generally results in high cooling rates due to the short laser/material interaction time due to high scanning speeds and high thermal gradients. This might lead to the formation of non-equilibrium phases such as glasses, quasi crystalline phases and new crystalline phases with extended composition ranges [3]. Finer structures may be observed in the microstructure at sufficiently high cooling rates compared to conventional manufacturing methods. Moreover, gas bubbles can become entrapped in the material during solidification due to various causes such as decrease in the solubility of the dissolved elements in the molten pool during cooling and solidification, chemical reaction or trapped gas [3]. Many material properties, such as yield strength, thermal conductivity or ductility highly depend on microstructural properties. One of the most striking examples of a structure-sensitive property is the fracture toughness which measures the ability of a structural material to inhibit crack propagation. Very small changes in the chemical composition and highly localized grain boundary segregation may cause a catastrophic loss of ductility [4]. Thus, the mechanical properties of SLM parts do not only depend on material composition, but also on the microstructures obtained and the presence of defects in the final product that are determined by the process parameters and manufacturing strategy [5].

The mechanical properties obtained with SLM and other layer manufacturing processes are widely studied by many research groups in the world. At the University of Leuven, the mechanical properties (hardness, tensile and bending properties) of SLM samples from Ti-6Al-4V materials were studied concluding that the obtained mechanical properties of SLM samples are comparable to those of bulk material [6]. Paul et al. reports about an investigation of laser rapid manufacturing of Inconel-625 components by the Taguchi method. They used tensile and impact tests in order to study the effects of different processing parameters, such as powder feed rate, scan speed and laser power [7]. In the field of Laser-Engineered Net Shaping (LENS™), mechanical properties of Ti-6Al-4V are investigated with tension, fatigue and crack-growth tests. The tests indicate that the static tensile strength and ductility, fatigue strength and fracture toughness of hot isostatic pressurized (HIP) parts produced via LENS™ compare favorably to those of wrought products [8]. The mechanical properties of pure titanium models processed by SLM are also investigated [9] showing that the impact and torsional fatigue strengths are low because of porosity and oxygen pick-up although the tensile strength tests show results comparable to the wrought material. There are also some investigations for other layer manufacturing processes such as for stereolithography [10] and selective laser sintering [11] [12]. In the field of rapid prototyping, a computer tool is also developed to simulate the mechanical properties of scaffolds for tissue engineering as a function of the pore size and selected material [13][11].

In this research, Charpy impact tests are applied to samples that were produced by SLM from three different metallic powders; a titanium alloy (Ti-6Al-4V) which is commonly used for medical applications, stainless steel 316L (X2CrNiMo18-14-3) and maraging steel 300 (X3CoMoTi18-9-5). The influence of various heat treatments applied on the samples after SLM process is investigated as well as the effect of the building axis. Hardness measurements are also conducted and the microstructures of the specimens have been analyzed.

2 EXPERIMENTAL PROCEDURE

Each of three materials was processed on a different machine. The stainless steel 316L is processed on a Concept Laser M3 Linear machine which employs an Nd:YAG laser with a wavelength of 1064 nm and a maximum laser output power of approximately 100 W measured in continuous mode. The specimens from maraging steel 300 were produced on an EOSINT M 270 machine. It employs a Yb-fibre laser with a maximum power of 195 W. The third powder material, titanium alloy Ti6Al4V, is processed on a self-made SLM machine at the University of Leuven (See Table 1). All specimens were manufactured with the selection of optimized parameters for density and roughness at the University of Leuven and LayerWise.

Table 1: Materials and machines used in this study

Powder	Maraging Steel	AISI 316 L	Ti-6Al-4V
Machine used	EOSINT M270 Yb-Fibre laser 195 W	Concept Laser M3 Linear Nd:YAG laser 100 W	Self-made LM machine Yb:YAG fibre laser 300 W

The Charpy impact test is used to determine material toughness by hitting a test specimen with a hammer, mounted at the end of a pendulum [14] (See Figure 2a). The specimen is broken by a single blow from a pendulum that strikes the middle of the specimen on the un-notched side. The height of rise subtracted from the height of fall gives the amount of energy absorption involved in deforming and breaking the specimen [15]. A V-shaped notch is generally used in the impact specimen in order to control the fracture process by concentrating stress in the area of minimum cross-section. In this experimental study, Charpy tests are done according to ASTM E23 standard [14]. The size of the standard specimen is 10 x 10 x 55 mm with a notch as defined in the same standard.

In this study, the experimental procedure was the same for all specimens. First, the samples were made by SLM process (See Figure 2b) and then they were cut off the base plate by electro-discharge machining (EDM). Due to the process, the loose powder that should stay as un-molten around the scanned contours sometimes melts and sticks to the part walls. In order to remove these loosely sticking powder particles, all produced samples were treated with sand blasting. Afterwards, the densities of the parts were measured with Archimedes method. The next step was to apply the impact test at room temperature if no heat treatment was applied. Otherwise, the parts were first treated in a furnace with an argon atmosphere according to a certain heat treatment cycle. After the impact test, the broken surfaces and the parts' insides were analyzed for their fracture surfaces and microstructures. Vickers hardness measurements were also conducted.

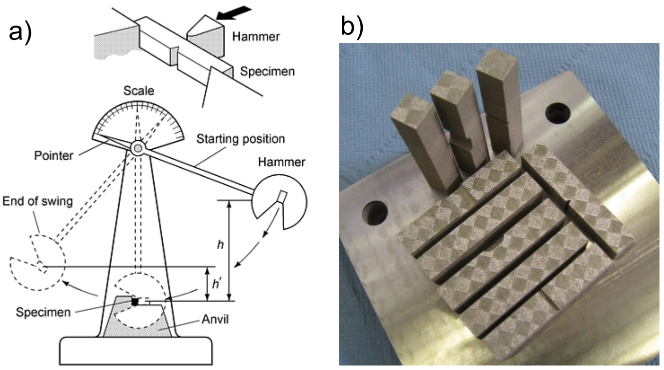

Figure 2: a) Charpy impact test setup [15] b) Produced specimens by SLM in three building axes

The experimental layout for all the batches produced is given in Table 2 where the number of produced samples from each material and specimen design is shown. Three batches of specimens from two materials (Ti alloy and the maraging steel 300) are produced in order to investigate different factors that may influence the toughness of SLM parts. Only 1 batch was produced in stainless steel 316L. In the first batch, two part designs are used to study whether high roughness values encountered in SLM cause any notch-effect influencing toughness results. Different part designs used in the experiments are shown in Figure 3a. A part design without a notch (design: 'no notch') but with an equal cross-section area is utilized as well as a standard Charpy test specimen (design: 'standard'). In the second batch, the influence of the building axis is taken under investigation with three part designs: the coordinate system attached to the part is shown in Figure 3b. In addition to the two designs explained above, a bar without any groove or notch is made, in which the notch defined by the standard is made afterwards by EDM (design: 'notch to be made by EDM'). Finally, in the third batch, standard specimens are produced along x-axis to test how different heat treatments may influence the toughness of SLM materials. For each material, different heating cycles are applied. The details of the heating cycles are explained in Section 3.3.

Table 2: The experimental layout

		AISI 316 L	Ti-6Al-4V	Maraging Steel
BATCH 1				
SPECIMEN DESIGN	Standard specimen	3	3	3
	No notch specimen	3	3	3
	EDM-notch specimen	no	no	no
	Building axis	x-axis	x-axis	x-axis
	Heat Treatment	none	none	none
	Sand Blasting	yes	yes	yes
	Number of replicates	3	3	3
BATCH 2				
SPECIMEN DESIGN	Standard specimen		3	3
	No notch specimen		3	3
	EDM-notch specimen		3	3
	Building Axis		x, y and z	x, y and z
	Heat Treatment		none	yes
	Sand Blasting		yes	yes
	Number of replicates		1	1
BATCH 3				
SPECIMEN DESIGN	Standard specimen		6	6
	No notch specimen		no	no
	EDM-notch specimen		no	no
	Building Axis		x-axis	x-axis
	Heat Treatment		2 types	2 types
	Sand Blasting		yes	yes
	Number of replicates		3	3

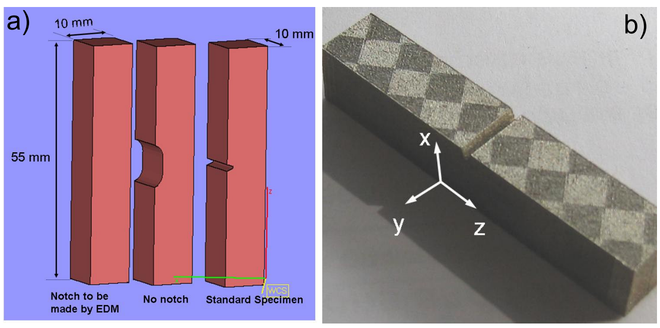

Figure 3: a) Three part designs produced by SLM to be used in Charpy tests b) Orientation of a standard part manufactured with the building axis coinciding x-direction

3 EXPERIMENTAL RESULTS

3.1 *First Batch*

As given in Table 2, none of the specimens were heat treated after the first batch. In order to check the repeatability of the process, 3 replicates for each specimen design and material were produced with a building direction parallel to the x-axis of the specimen.

The cross section of the parts is shown in Figure 4. The stainless steel 316L part consists mainly of an austenitic phase, as revealed by X-Ray Diffraction. The cellular microstructure looks similar to the structure obtained after casting of austenitic stainless steel: delta ferrite in an austenitic matrix. The micro-Vickers hardness (0,5 kg) is 235 ± 5. The Ti-6Al-4V parts consist of large grains oriented along the building direction. The elongated grains are the result of epitaxial solidification and extend over multiple layers. Inside the grains a needle-like martensitic phase, which is formed as a result of the rapid solidification, can be distinguished instead of the two-phase hcp alfa and bcc beta structure that would be present in equilibrium conditions. The micro-Vickers hardness is 369 ± 5. The structure of the maraging steel parts is mainly a low carbon bcc lath martensitic structure. The borders of the melt pools are revealed after etching. The micro-Vickers hardness is 376 ± 5.

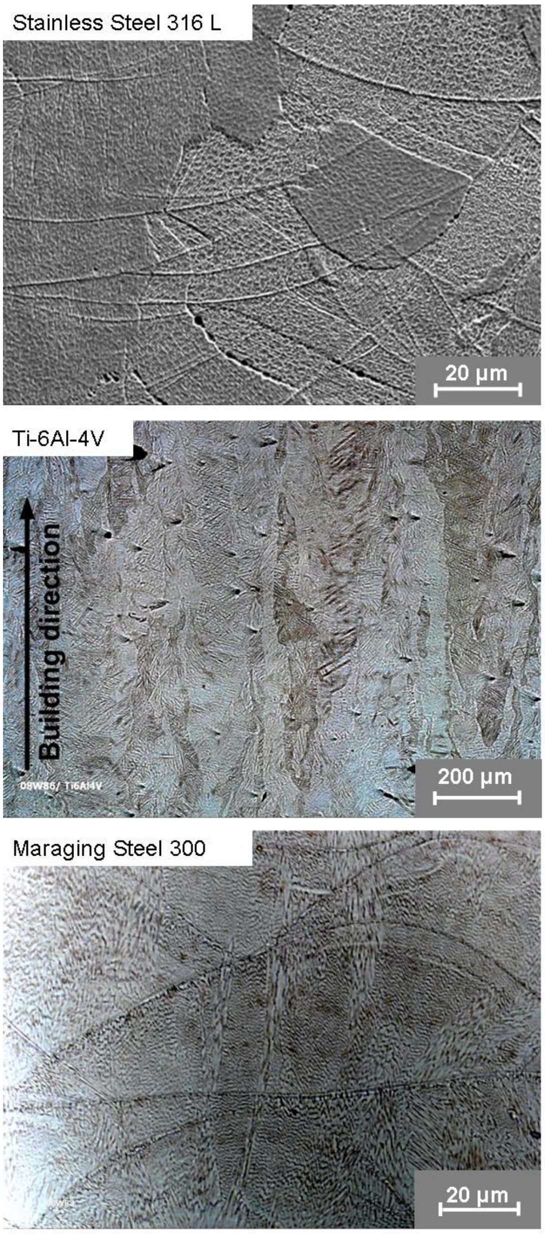

Figure 4: Micrographs of etched SLM parts

The density measurements and Charpy test results are presented in Figure 5 and Figure 6, respectively. The results shown in all figures are given with a 95% level of confidence. The theoretical densities for 316L, Ti6Al4V and the maraging steel 300 are taken as 8.0, 4.2 and 8.1 g/cm^3, respectively. Figure 5 depicts that all specimens have relative densities of more than 98.5%.

The Charpy test results show that the specimens of the same material with and without a notch absorb quite different energy values before breakage. For all materials, the specimens with a notch have less resistance to breakage which means that the high roughness of the SLM process does not behave like stress-concentrating notches. Both specimen designs follow the same trend for three materials. The maraging steel 300 and 316L stainless steel show more or less similar results whereas Ti alloy has much less toughness than steel for both designs.

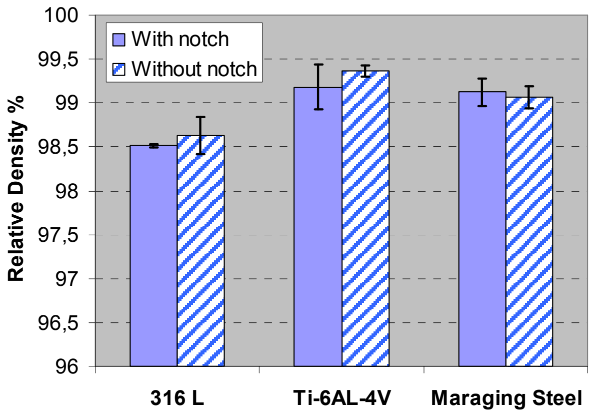

Figure 5: The density measurement results of the first batch specimens by Archimedes method

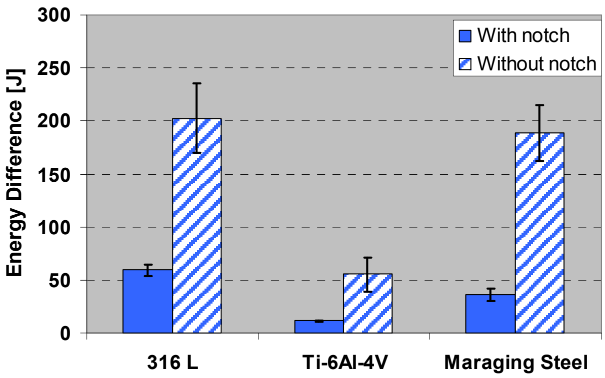

Figure 6: The Charpy test results for SLM produced parts for the first batch

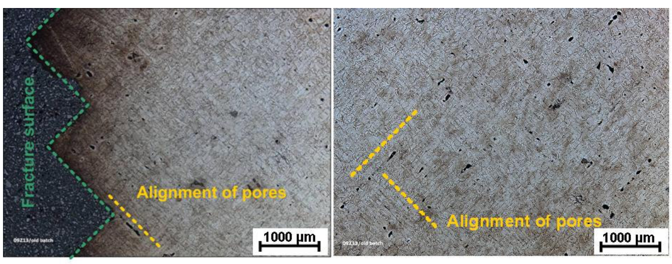

Figure 7: Cross section of stainless steel 316L perpendicular to the building direction after Charpy testing.

The stainless steel specimens have a waved fracture surface. Figure 7 shows that the waviness is a result of aligned pores along which fracture has occurred. Pores containing incompletely molten particles are present on all fracture surfaces, as illustrated in Figure 8.

Fracture of the Ti-6Al-4V parts is mainly brittle as indicated by the minor deformation of the cross section at the position of fracture (see Figure 9). The maraging steel parts behave in a more ductile behavior as indicated by the higher deformation and presence of larger shear lips.

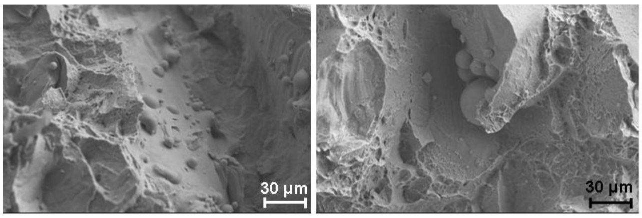

(a) AISI 316L b) Ti-6Al-4V

Figure 8: SEM investigation of fracture surface

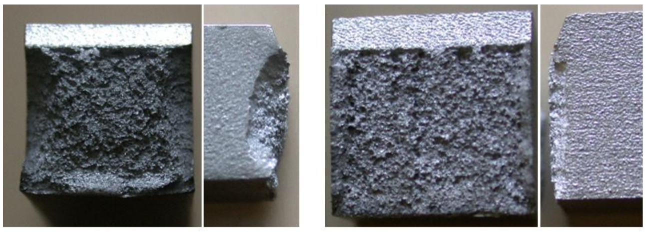

a) Maraging Steel b) Ti-6Al-4V

Figure 9: Top (at the left) and side (at the right) view of SLM parts after Charpy testing

3.2 *Second Batch*

As shown in Table 2, the second batch is performed to investigate the effect of the building axis on the Charpy test results for SLM parts. In order to determine the influence for different notch making methods, all three specimen designs were produced. Only one specimen was manufactured per each case. No heat treatment is applied for Ti alloy whereas solution annealing followed by aging is applied to maraging steel 300 specimens since it is a material which is always used with a heat treatment.

The results derived with the two materials exhibited similar results obtained with the specimens produced in the first batch when the same building axis and same design geometries are considered. For the Ti alloy, although the specimens built along y-axis showed a slightly higher resistance to breakage, the effect of the building axis seems negligible as seen in Figure 10. The same holds true for the maraging steel of which the results are given in Figure 11, where the weakest building direction seems to be the x-axis for the specimens without notch. It can be concluded that in case of a good connection between successive layers without any pores, the building axis does not play a significant role in the toughness results. As also observed from the macro pictures of the broken surfaces, all specimens made along x, y and z have similar brittle fracture. The reason for low toughness of z-specimens made of Ti alloy can be attributed to porosity caused by the accidental reduction of laser power (about 5%) during the build of z-specimens. The protection glass that is located between the vacuum chamber and the lens became dirty as the build height increases and this caused the undesired reduction in the power leaving an extra porosity of 2% in the samples.

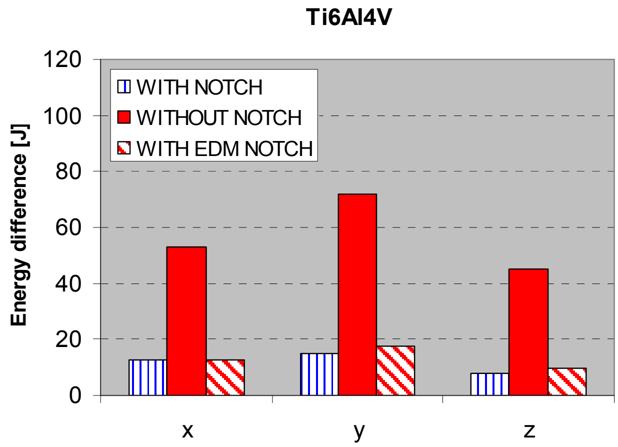

Figure 10: The Charpy results of the Ti alloy in the second batch

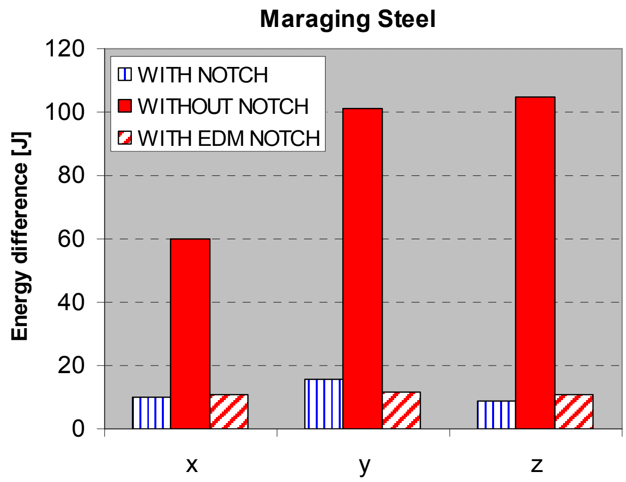

Figure 11: The Charpy results of the maraging steel 300 in the second batch

3.3 *Third Batch*

The influence of various heat treatments on the toughness of two materials is investigated in this batch. All specimens with a standard design are produced along x-axis with three replicates for each case.

For the Ti alloy, two different heat treatments were applied. The first one was the full annealing conducted at 735 °C for 2 hours in a BIP argon furnace. The second heat treatment was the stress relieving at 595 °C for 3 hours in an argon atmosphere. The first heat treatment did not improve or worsen the toughness of this material, the hardness was slightly increases (362 ± 9). The second heat treatment decreased the toughness of Ti alloy slightly and significantly increases the hardness to 386 ± 5 (See Figure 12). During heat treatment the martensitic structure transforms into a mixture of hcp alfa and bcc beta phases. The lower Charpy energy after heat treatment at 595°C may be attributed to the higher amount of less ductile alfa phase present than after heat treatment at 735°C.

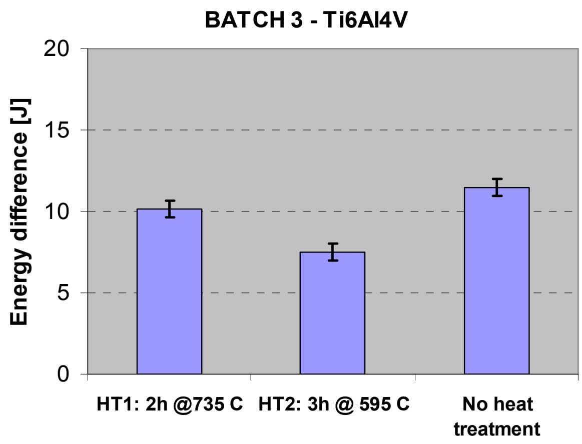

Figure 12: The Charpy results of Ti alloy for full annealing and stress relieving compared to not heat treated parts (third batch)

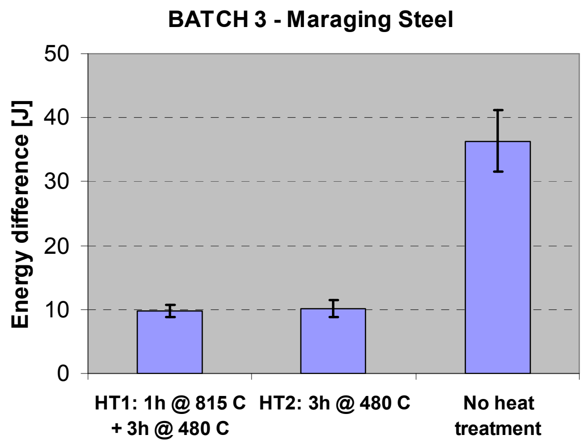

Figure 13: The Charpy results of the maraging steel for solution annealing followed by aging and only aging compared to not heat treated parts (third batch)

For the maraging steel, the applied two heat treatments decrease the resistance to breakage significantly as depicted in Figure 13. It can also be observed that the amount of plastic deformation is significantly lower than without heat treatment. The first heat treatment was the solution annealing at 815 °C for 1 hour and cooling to room temperature followed by aging conducted at 480°C for 3 hours. The second was only aging at 480 °C for 3 hours. The results also show that the solution annealing is not necessary to homogenize the microstructure after SLM process since the results with and without solution annealing were almost the same. The hardness increases to 572 ± 7 as a result of aging. The hardening during aging has been attributed in literature to short-range ordering in the cobalt-bearing solid solution and the precipitation of nickel-rich intermetallic compounds in the lath martensitic structure [16]. X-ray diffraction has revealed that after aging a fcc phase appears, which was not present without heat treatment. In literature, it is reported that during aging of 18 Ni maraging steel 300 austenite can precipitate and adversely affect the toughness of the material [16].

4 COMPARISON OF TOUGHNESS OF SLM PARTS AND BULK MATERIAL

The toughness of bulk materials is higher than that of SLM parts. For bulk annealed stainless steels, the impact Charpy energy for V-notched parts is generally greater than 130 J [16]. For Ti-6Al-4V, cast specimens exhibit an impact energy of 15 J for V-notched samples [18] whereas SLM parts reach up to 11.5 J without any heat treatment in the present work. After full annealing or stress relieving, the toughness does not change or slightly decreases. Bulk maraging steel 300, i.e. a pre-alloyed high strength and hardness steel, has an impact energy of 18 J at room temperature after aging [18]. Our experiments showed an impact energy of approximately 10 J for this material when heat treated in the same way. Without any heat treatment, the impact energy is found to be between 30 to 40 J, thus yielding a higher toughness but sacrificing the strength and hardness normally obtained through aging. The comparison between test results of SLM and conventional manufacturing processes is summarized in Table 3. The reason of having lower toughness with SLM can be attributed to the presence of defects like pores, pick-up of impurities like oxygen and nitrogen (especially for titanium alloys) and the presence of more brittle non-equilibrium phases.

Table 3: Comparison of SLM and conventional processes in terms of Charpy V-notch toughness

	SLM	Conventional
Ti-6Al-4V	11,5 ± 0,5 J (as built) 10,1 ± 0,5 J (full annealed)	15 J for investment casting
Maraging Steel 300	36,3 ± 4,8 J (as built) 10,1 ± 1,4 J (after aging)	18 J after aging
Stainless Steel 316 L	59,2 ± 3,9 J (as built)	160 J for cast CF-3M after annealing

Tests which were not presented in this paper revealed that the porosity of SLM parts is of high importance since it might cause a significant reduction in toughness. Controlling the process in terms of density is hence most critical: a slight drop of density due to unexpected loss of laser energy (e.g. dirt on optics) may substantially reduce the toughness (typically 20% for less than 1% reduction in density measured with optical microscopy picture analysis). Testing density should best be done with different methods since Archimedes may overestimate the relative density if the pores still contain un-molten powder particles. In terms of stainless steel, a slight change of alloying element compositions may significantly reduce the toughness due to undesired phases such as high temperature delta ferrites in the austenite phase. Thus the material composition should also be strictly determined to ensure a good repeatability.

5 CONCLUSIONS

One of the important conclusions from the experiments conducted in this study is the fact that the roughness of SLM parts does not behave like stress-concentrating notches. The parts without a notch showed significantly higher impact energies compared to specimens with a notch, either made during the SLM process or after SLM by EDM. This also concludes that the way of production of the notch does not affect the toughness results. Additionally, the specimens made in the second batch revealed that the building axis does not play an important role on the toughness results if the connection between successive layers is well established without any directional porosity.

6 ACKNOWLEDGEMENTS

The authors acknowledge K.U.Leuven for support through the project GOA/2002-06, IWT for support through the SBO-project DiRaMaP and TUBITAK (The Scientific and Technological Research Council of Turkey) for financial support to Evren Yasa under “Ph.D. support program for students in foreign countries”.

7 REFERENCES

[1] Kruth, J.-P., Vandenbroucke, B., Van Vaerenbergh, J., Mercelis, P., Benchmarking of different SLS/SLM processes as rapid manufacturing techniques, In Proceedings of Int. Conf. Polymers and Moulds Innovations (PMI), Gent, Belgium, April 20-23, 2005.

[2] Yadroitsev, I., Bertrand, Ph., Smurov, I., 2007, Parametric analysis of the selective laser melting process, Applied Surface Science, 253, pp.8064-8069.

[3] Rombouts, M., Selective Laser Sintering/Melting of iron-based powders, Ph.d. Thesis, Katholieke Univesiteit Leuven, 2006.

[4] Brandon, D. and Kaplan, W.D., 2001, Microstructural Characterization of Materials, 2nd edition, published in Great Britain, John Wiley & Sons Ltd.

[5] Yadroitsev, I., Thivillon, L., Bertrand, Ph., Smurov, I., 2007, Strategy of manufacturing components with designed internal structure by selective laser melting of metallic powder, Applied Surface Science, 254, pp.980-983.

[6] Vandenbroucke, B., Kruth, J.-P., 2007, Selective Laser melting of biocompatible metals for rapid manufacturing of medical parts, Rapid Prototyping Journal,13/4, pp.196-203.

[7] Paul, C.P., Ganesh, P., Mishra, S.K., Bhargava, P., Negi, J., Nath, A.K., 2007, Investigating laser rapid manufacturing for Inconel-625 components, Optics and Laser Technology, 39, pp.800-805.

[8] Kobryn, P.A., Semiatin, S.L., 2002, Mechanical properties of laser-deposited Ti-6Al-4V, in Proc. of SFF conference 2002, Austin, Texas, USA..

[9] Santos, E., Abe, F., Kitamura, Y., Osakada, K., Shiomi, M., 2002, Mechanical properties of pure titanium models processed by selective laser melting, in Proc. of SFF conference 2002, Austin, Texas, USA.

[10] Saleh, N., Mansour, S., Hague, R., 2002, Investigation into the mechanical properties of rapid manufacturing materials, in Proc. of SFF conference, Austin, Texas, USA.

[11] Miani, F., Kuljanic, E., Sortino, M., 2001, Modelling the mechanical properties of direct metal selectively laser sintered parts, In Proc. Laser Assisted Net Shape Engineering 3, LANE 2001, Germany.

[12] Hague, R.J., Dickens, P.M., Mansour, S., Saleh, N., and Sun, Z., 2002, Design for Rapid Manufacture, Proceedings of the Society of Rapid Manufacturing Engineers’ Rapid Prototyping and Manufacturing Conference, Cincinnati, USA [CD ROM].

[13] Almeida, H.A., Bartolo, P.J., Ferreira, J.C., Mechanical behavior and vascularisation analysis of tissue engineering scaffolds, Virtual and Rapid Manufacturing, Taylor and Francis Group, London, 2008, pp.71-80.

[14] ASTM, E 23-96, Standard Test Methods for Notched Bar Impact Testing of Metallic Materials.

[15] ASM handbook: Material Selection and Design, Vol. 20, 1997, ISBN 0-87170-386-6.

[16] ASM handbook: Heat Treating, Vol. 4, 1991, ISBN 0-87170-379-3.

[17] www.interalloy.com.au/data_sheets/stainless_steel

[18] http://www.kubotametal.com/alloys/corrosion_resistant/CF-3M.pdf

[19] Latrobe Specialty Steel Company, www.latrobesteel.com, MARVAC™ 300 VIM-VAR Data-sheet